

# Amphipathic $\alpha$ -Helix Bundle Organization of Lipid-Free Chicken Apolipoprotein A-I<sup>†</sup>

Robert S. Kiss,<sup>‡</sup> Cyril M. Kay,<sup>§</sup> and Robert O. Ryan<sup>\*,‡</sup>

*Lipid and Lipoprotein Research Group and Protein Engineering Network of Centres of Excellence (PENCE), Department of Biochemistry, University of Alberta, Edmonton, Alberta, Canada T6G 2S2*

*Received November 2, 1998; Revised Manuscript Received January 25, 1999*

**ABSTRACT:** Apolipoprotein A-I (apoA-I), the major protein component of plasma high-density lipoprotein (HDL), exists in alternate lipid-free and lipid-bound states. Among various species, chicken apoA-I possesses unique structural properties: it is a monomer in the lipid-free state and it is virtually the sole protein component of HDL. Near-UV circular dichroism (CD) spectroscopic studies provide evidence that chicken apoA-I undergoes a major conformational change upon binding to lipid, while far-UV CD data indicate its overall  $\alpha$ -helix content is maintained during this transition. The fluorescence emission wavelength maximum (excitation 295 nm) of the tryptophans in apoA-I (W74 and W107) displayed a marked blue shift in both the lipid-free (331 nm) and HDL-bound (329 nm) states, compared to free tryptophan in solution. The effect of aqueous quenchers on tryptophan fluorescence was determined in lipid-free, dimyristoylphosphatidylcholine (DMPC)- and HDL-bound states. The most effective quencher in the lipid-free and HDL-bound states was acrylamide, giving rise to  $K_{sv}$  values of  $1.6 \pm 0.1$  and  $1.2 \pm 0.1$  M<sup>-1</sup>, respectively. Together, these data suggest that a hydrophobic environment around the two tryptophan residues (W74 and W107) is maintained in alternate conformations of the protein. To further probe the molecular organization of lipid-free apoA-I, its effect on the fluorescence properties of 8-anilino-1-naphthalenesulfonic acid (ANS) was determined. Human and chicken apoA-I induced a similar increase in ANS fluorescence quantum yield, in keeping with the hypothesis that these proteins adopt a similar global fold in the absence of lipid. When considered with near- and far-UV CD experiments, the data support a model in which lipid-free chicken apoA-I is organized as an amphipathic  $\alpha$ -helix bundle. In other studies, lipid-soluble quenchers, 5-, 7-, 10-, and 12-DOXYL stearic acid (DSA), were employed to investigate the depth of penetration of apoA-I into the surface monolayer of spherical HDL particles. 5-DSA was the most effective quencher, suggesting that apoA-I tryptophan residues localize near the surface monolayer, providing a structural rationale for the reversibility of apoA-I–lipoprotein particle interactions.

Apolipoprotein (apo)<sup>1</sup> A-I is a 28 kDa exchangeable apolipoprotein that plays an important role in plasma cholesterol homeostasis (1). ApoA-I activates the enzyme lecithin:cholesterol acyltransferase and serves as the major structural component of high-density lipoprotein (HDL). As a lipid-poor protein, apoA-I mediates removal of cholesterol from peripheral tissues, facilitating its return to the liver via the reverse cholesterol transport pathway (2, 3). This pathway is believed to be responsible for the inverse correlation between HDL levels and risk of cardiovascular disease (4).

Recently, the three-dimensional structure of N-terminal truncated human ( $\Delta 1$ –43)apoA-I has been elucidated at 4 Å resolution (5). The structure clearly depicts the preponderance of amphipathic  $\alpha$ -helices in the protein and suggests a possible molecular organization of lipid-bound apoA-I. It is conceivable that antiparallel dimers of apoA-I form an extended “belt” around the periphery of spherical lipoproteins or bilayer disk complexes with hydrophobic regions of the protein in direct contact with the lipid surface. At the same time, important questions remain about the conformation of full-length apoA-I in the absence of lipid and the nature of lipid binding-induced structural adaptations.

Several approaches have been used to study the structure–function relationship of human apoA-I, including spectroscopic studies (6, 7), deletion mutants (8), N- and C-terminal truncation (9–12), and helix-swapping mutagenesis (13). Other approaches include study of HDL recombinants containing only apoA-I (14–16). Despite these efforts, the molecular basis for dual existence of apoA-I in lipid-poor and lipid-associated states remains unclear. The characteristic property of human apoA-I to oligomerize in the absence of

<sup>†</sup> Supported by grants from the Medical Research Council and the Alberta Heart and Stroke Foundation. R.S.K. is supported by a research traineeship from the Heart and Stroke Foundation of Canada.

\* Address correspondence to this author at 328 Heritage Medical Research Centre, University of Alberta, Edmonton, Alberta, Canada T6G 2S2. Fax: (780) 492-3383. Email: robert.ryan@ualberta.ca.

<sup>‡</sup> Lipid and Lipoprotein Research Group.

<sup>§</sup> Protein Engineering Network of Centres of Excellence (PENCE).

<sup>1</sup> Abbreviations: apo, apolipoprotein; HDL, high-density lipoprotein; CD, circular dichroism; DMPC, dimyristoylphosphatidylcholine; ANS, 8-anilino-1-naphthalenesulfonic acid; DSA, DOXYL stearic acid; TFE, trifluoroethanol.

lipid over a broad concentration range (17–19) suggests hydrophobic lipid binding sites in this protein may be protected from solvent exposure through formation of intermolecular helix–helix contacts.

ApoA-I from chicken plasma shares 48% sequence identity and 68% sequence homology with human apoA-I (as determined by the SEQSEE sequence homology program; 20). Unlike human apoA-I, chicken apoA-I is monomeric in the lipid-free state over a broad concentration range and comprises >95% of the protein component of chicken HDL (21, 22). Circular dichroism (CD) studies reveal lipid-free chicken apoA-I possesses an exceptionally high  $\alpha$ -helix content (22, 23) while sequence analysis indicates helical segments are amphipathic (24). These features suggest that chicken apoA-I is a good candidate for structure–function studies, including study of lipid binding-induced conformational changes. In this regard, chicken apoA-I contains two tryptophan residues, at positions 74 and 107. Both tryptophans are centrally located in the protein sequence and are predicted to reside on the hydrophobic face of distinct amphipathic  $\alpha$ -helices.

In the present study, spectroscopic techniques have been used to examine different conformational states of chicken apoA-I. Near-UV CD studies provided evidence for a conformational change upon lipid association while far-UV CD data indicate the protein retains its high content of  $\alpha$ -helix secondary structure in either state. Water-soluble and lipid-based quenching agents have been employed to monitor the microenvironment of apoA-I tryptophan residues in different conformational states. The results are consistent with organization of lipid-free apoA-I as a helix bundle. Furthermore, the data indicate that chicken apoA-I adopts a relatively superficial association with the HDL phospholipid monolayer. The ramifications of these results in terms of the physiological role of apoA-I in lipoprotein metabolism are discussed.

## EXPERIMENTAL PROCEDURES

**Materials.** 5-, 7-, 10-, and 12-DOXYL stearic acid (DSA) were obtained from Aldrich (St. Louis, MO). 8-Anilino-1-naphthalenesulfonic acid (ANS), dimyristoylphosphatidylcholine (DMPC), and trifluoroethanol (TFE) were purchased from Sigma Chemical Co. (St. Louis, MO). All other chemicals were of analytical grade.

**Lipoproteins and Apolipoproteins.** Chicken HDL and apoA-I were prepared as described by Kiss et al. (22). Human apoA-I was prepared according to Yokoyama et al. (25). ApoA-I/DMPC disks were prepared by the cholate dialysis method (26) with a lipid to protein weight ratio of 2.5 to 1 (w/w). The disk preparation was adjusted to a density of 1.21 g/mL and subjected to ultracentrifugation in a VTi 65.2 rotor at 65 000 rpm for 1.1 h at 4 °C to separate unbound apolipoprotein.

**Circular Dichroism Experiments.** A Jasco J-720 spectropolarimeter (Jasco Inc., Easton, MD) connected to a Epson Equity 386/25 computer was used to obtain circular dichroism (CD) measurements. Samples were kept at constant temperature (25 °C) by a thermostated cell holder connected to a circulating water bath (Lauda, Westbury, NY). The instrument was calibrated regularly with ammonium *d*-(+)-10-camphorsulfonate at 290.5 and 192 nm and with *d*-(-)-

pantoyllactone at 219 nm. The average of 10 scans was used to increase the signal-to-noise ratio, and smoothing was employed to remove the high-frequency noise. Distortion of CD spectra was minimized by keeping the voltage of the photomultiplier below 500 V. The cell used for wavelengths below 250 nm was 0.02 cm (calibrated for cell length). Far-UV spectra were obtained using protein concentrations between 0.5 and 1.0 mg/mL. Near-UV spectra were obtained using a protein concentration of 1.0 mg/mL with a 1.0 cm microcell. Modified Provencher–Glöckner analysis using the Contin program (Version 1.0) gave predictions of secondary structure from the CD data (27), and, as such, may give slightly different values than those previously published (22).

**Spectroscopy.** Fluorescence spectroscopy was performed on an LS 50 luminescence spectrometer (Perkin-Elmer, Beaconsfield, England). All measurements were conducted at 24 °C with the excitation and emission slit widths set at 5 nm. Increasing concentrations of quenchers were added to the protein sample, and tryptophan emission spectra were obtained (295 nm excitation). KI solutions contained 1 mM sodium thiosulfate to suppress free iodide formation (28). A correction for the inner filter effect was taken into account when using acrylamide (29). Concentrations of fatty acid spin-labels were determined by electron spin resonance. Fluorescence intensity values were corrected for dilution effects. The effective Stern–Volmer quenching constants ( $K_{sv}$ ) for aqueous quenchers in lipid-free and lipid-bound states were calculated (29).  $K_{sv}$  values were calculated from the equation  $F_0/F = 1 + K_{sv}[Q]$ , where  $F_0$  and  $F$  are corrected fluorescence measurements at the emission maximum wavelength in the absence and presence of quencher, respectively, and  $[Q]$  is the concentration of quencher. A plot of  $F_0/F$  vs  $[Q]$  yields a straight line, whose slope is  $K_{sv}$  (30). Values are the average of three independent measurements  $\pm$  SD. In the case of spin-labeled fatty acids, the Stern–Volmer equation does not apply since the quencher is not uniformly distributed throughout the unit volume (30–32). We have, therefore, computed apparent Stern–Volmer quenching constants ( $K_{app}$ ) for the purposes of comparison.

8-Anilino-1-naphthalenesulfonic acid (ANS) fluorescence emission spectra were obtained in the presence of human and chicken apoA-I (50  $\mu$ g/mL, 1.8  $\mu$ M). 250  $\mu$ M ANS in 10 mM sodium phosphate buffer (pH 7.5) was excited at a wavelength of 395 nm with slit widths of 5 nm. Since ANS fluorescence in buffer is negligible (33), spectra were recorded in the presence of a minimum 100-fold excess of ANS with respect to protein (mol/mol). Carbonic anhydrase (50  $\mu$ g/mL, 1.8  $\mu$ M), a globular, water-soluble protein, served as a negative control. Bovine serum albumin (50  $\mu$ g/mL, 0.7  $\mu$ M), known to have hydrophobic binding pockets, was employed as a positive control.

**Analytical Ultracentrifugation.** Sedimentation velocity runs were carried out at 20 °C and 50 000 rpm using a Beckman XLI analytical ultracentrifuge and absorbance optics following the procedures outlined in the instruction manual published by the Spinco Business Center of Beckman Instruments, Inc., Palo Alto, CA (1997). Runs were performed for 4 h during which a minimum of 20 scans were taken. The sedimentation velocity data were analyzed using the Transport Method contained in the Beckman Analysis Program [Optima XL-A/XL-I Data Analysis Software, Version 4.0 Copyright (c) 1997]. The program Sednterp

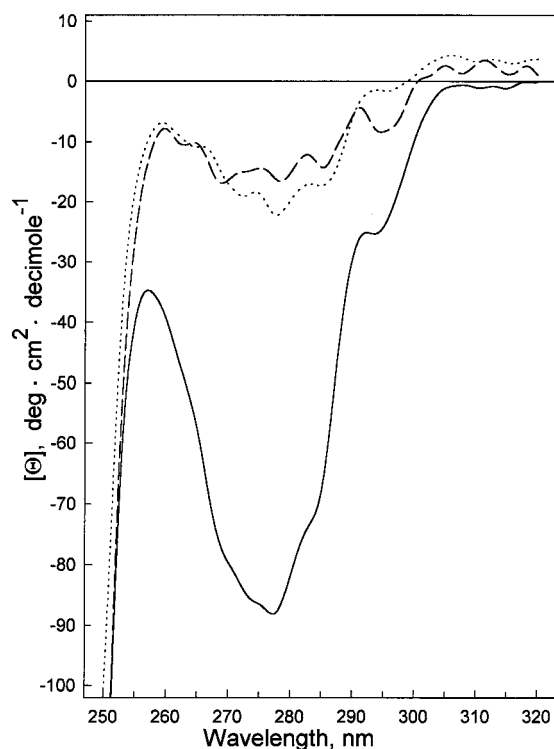


FIGURE 1: Near-UV CD spectra of lipid-free apoA-I (straight line), DMPC-bound apoA-I (dashed line), and HDL-bound apoA-I (dotted line).

(Sedimentation Interpretation Program, Version 1.01) was used to calculate the intrinsic sedimentation constant,  $s_{20,w}^0$ , the frictional ratio,  $f/f_0$ , and the axial ratio,  $a/b$ . Sednterp calculates the partial specific volume and degree of hydration from the amino acid composition of the protein using the methods of Cohn and Edsall (34) and Kuntz (35), and also calculates the solvent density and viscosity using known values from physical tables. The density and viscosity of TFE were taken into account for the calculation of  $s_{20,w}^0$  in that solvent, and the partial specific volume and degree of hydration were assumed not to change upon addition of TFE, a finding noted by MacPhee et al. (36) in studies of the effect of TFE on the solution behavior of amphipathic peptides.

## RESULTS

**Circular Dichroism Spectroscopy.** To evaluate conformational adaptations of lipid-free chicken apoA-I postulated to occur upon lipid binding, near-UV CD spectra were collected under different conditions (Figure 1). The spectrum of apoA-I in buffer was dominated by a contribution from the seven tyrosines in the protein, giving rise to an extremum at 278 nm. The shoulder at 295 nm can be attributed to the two tryptophans (W74 and W107). Little effect of the five phenylalanines in the protein was observed. Spectra of apoA-I bound to HDL or to DMPC disk particles differed significantly from the spectrum of lipid-free apoA-I. In addition to subtle differences in fine structure, the major spectral change corresponded to a large decrease in ellipticity in the region between 260 and 290 nm, indicative of a conformational change upon lipid binding (37, 38). As well, extrema for DMPC-bound apoA-I at 263, 270, and 293 nm were similar but slightly blue-shifted compared to HDL-bound apoA-I. This can be attributed to small differences in

the environment of some tyrosines and tryptophans, indicating that apoA-I conformations in DMPC- and HDL-bound states are similar, but nonetheless unique.

Far-UV CD spectra of chicken apoA-I in buffer alone or complexed to lipid particles (spherical HDL or DMPC disks) are generally similar, with major troughs at 208 and 222 nm [data not shown; see Kiss et al., (22)]. Modified Provencher–Glöckner analysis of spectral data indicates  $\alpha$ -helix is the predominant secondary structure component present in the different states, with minor amounts of other conformers (Table 1). Differences in  $\alpha$ -helix content between apoA-I bound to HDL versus DMPC disk particles suggest subtle differences in apoA-I conformation when associated with these morphologically and compositionally distinct lipid particles. The observation that  $\alpha$ -helix remains the predominant secondary structure element in both lipid-free and lipid-associated states is consistent with the hypothesis that amphipathic  $\alpha$ -helical segments in lipid-free apoA-I reposition upon lipid interaction, exposing hydrophobic sites which become available for contact with the lipid surface.

**Tryptophan Fluorescence Emission of Chicken ApoA-I.** Fluorescence spectra of apoA-I in buffer display an emission maximum at 331 nm, similar to that observed for DMPC disk complexes or HDL particles (Table 1). Compared to the emission wavelength maximum of free tryptophan in aqueous solution (347 nm), apoA-I tryptophan fluorescence emission is blue-shifted in all three states. Thus, in lipid-free and lipid-bound states, W74 and W107 reside in a hydrophobic environment, shielded from the aqueous milieu. Previous fluorescence studies of apoA-I from other species revealed that chicken apoA-I is distinctive in terms of the magnitude of the blue shift in its tryptophan fluorescence emission wavelength maximum (21). The observed blue shift in the absence of lipid indicates that monomeric apoA-I adopts a tertiary structure that maintains a hydrophobic environment in the vicinity of W74 and W107. Given the preponderance of amphipathic  $\alpha$ -helix in the protein, and precedent established from structural studies of other apolipoproteins (39–42), it is reasonable to consider that helix–helix interactions may serve to sequester the tryptophan residues. By extension, it is conceivable that lipid binding induces a conformational adaptation in apoA-I wherein helix–helix contacts are replaced by helix–lipid interactions, with presentation of helices containing W74 and W107 to the hydrophobic lipid milieu.

**Fluorescence Quenching Studies.** Three commonly used quenching agents, KI, CsCl, and acrylamide, were employed as aqueous quenchers of the intrinsic fluorescence of the two tryptophan residues in apoA-I. Figure 2 shows acrylamide quenching curves obtained for lipid-free, DMPC-bound, and HDL-bound apoA-I. Quenching curves obtained with KI and CsCl revealed small differences between the different states of apoA-I, noting that  $\text{Cs}^+$  was a particularly ineffective quenching agent (data not shown). Comparison of Stern–Volmer quenching constants for the different quenchers indicates similar accessibility in the lipid-free and lipid-bound states (Table 2). In the case of the neutral quenching agent acrylamide, the similar  $K_{sv}$  values obtained in the presence and absence of lipid suggest that lipid-free apoA-I adopts a fold that sequesters W74 and W107 from the aqueous environment. The observed increased ability of KI to quench apoA-I fluorescence in DMPC disks indicates that the



Table 1: Properties of Chicken ApoA-I

apoA-I	secondary structure conformers <sup>a</sup>				scale factor <sup>b</sup>	fluorescence emission $\lambda_{\text{max}}$ (nm) <sup>c</sup>
	$\alpha$ -helix (%)	$\beta$ -sheet (%)	$\beta$ -turn (%)	remainder (%)		
lipid-free	72 $\pm$ 2	8 $\pm$ 2	12 $\pm$ 1	9 $\pm$ 1	1.001	331
DMPC-bound	68 $\pm$ 2	7 $\pm$ 3	16 $\pm$ 1	9 $\pm$ 1	0.990	331
HDL-bound	86 $\pm$ 1	0 $\pm$ 0	8 $\pm$ 1	3 $\pm$ 1	0.997	329

<sup>a</sup> Values derived from modified Provencher–Glöckner analysis (27) of far-UV CD spectra as described in the text. The percentage error for the values was derived from the relative goodness-of-fit of the spectra in comparison to a standard set of 16 reference proteins plus poly(L-glutamate) (employed as a 100% helical reference). <sup>b</sup> Scale factor represents the goodness-of-fit and should theoretically be 1.0. <sup>c</sup> Wavelength of maximal fluorescence emission (excitation 295 nm).

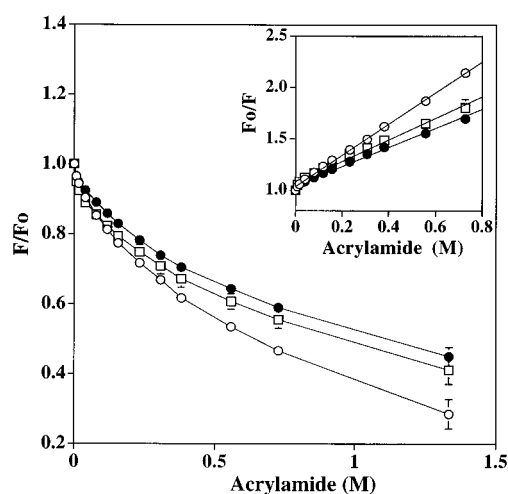


FIGURE 2: Fluorescence quenching of tryptophans by acrylamide. Increasing concentrations of acrylamide were added to a 50  $\mu$ g/mL solution of chicken apoA-I in the lipid-free (open circles), DMPC-bound (filled circles), and HDL-bound (open squares) states. Emission spectra were obtained from 300 to 450 nm with excitation at 295 nm (excitation and emission slit widths set at 5 nm). Relative fluorescence ( $F/F_0$ ) is plotted as a function of quencher concentration. Inset: Stern–Volmer plot of acrylamide quenching of apoA-I tryptophan fluorescence. Values are the average of three independent measurements  $\pm$  SD.

Table 2: Effective Stern–Volmer Constants ( $K_{sv}$ ) for Aqueous Quenchers

	$K_{sv}$ ( $M^{-1}$ ) <sup>a,b</sup>		
	lipid-free apoA-I	DMPC-bound apoA-I	HDL-bound apoA-I
CsCl	0.1 $\pm$ 0.0	0.1 $\pm$ 0.0	0.1 $\pm$ 0.0
KI	0.6 $\pm$ 0.1	1.3 $\pm$ 0.1	0.6 $\pm$ 0.0
acrylamide	1.6 $\pm$ 0.1	1.1 $\pm$ 0.1	1.2 $\pm$ 0.1

<sup>a</sup> Stern–Volmer quenching constants ( $K_{sv}$ ) for aqueous quenchers in lipid-free and lipid-bound states were calculated as described under Experimental Procedures. <sup>b</sup> Values reported represent the mean  $\pm$  SD of three separate determinations.

environment of the tryptophans is more accessible in the disk-bound state than in lipid-free or HDL-bound states. This result is consistent with interaction of the protein around the periphery of the bilayer disk as opposed to penetration between polar headgroups of the phospholipid, as proposed for spherical HDL particles (43).

**Dye Binding Experiments.** ANS is a dye whose intrinsic fluorescence increases upon binding to a hydrophobic surface or cavity (33). In the absence of protein, ANS has a very low quantum yield with an emission wavelength maximum of 515 nm (excitation 395 nm). Addition of either human or chicken apoA-I induced a significant enhancement in ANS

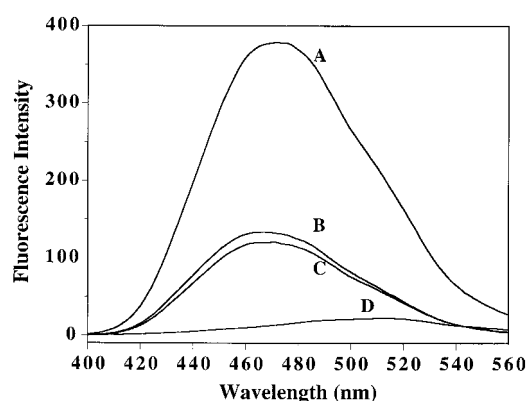


FIGURE 3: ANS fluorescence spectra were obtained in the presence of 50  $\mu$ g/mL bovine serum albumin (A), human apoA-I (B), chicken apoA-I (C), and carbonic anhydrase (D). Protein samples were excited at 395 nm and the emission spectra from 400 to 560 nm monitored (excitation and emission slit widths set at 5 nm). Spectra were recorded in 10 mM sodium phosphate (pH 7.5).

fluorescence quantum yield together with a 35 nm blue shift in its wavelength of maximum emission (Figure 3). The comparable induction of fluorescence elicited by human and chicken apoA-I suggests the relative amount of ANS-accessible hydrophobic surface in these proteins is similar. Bovine serum albumin induced a large enhancement in ANS fluorescence spectra, consistent with the known hydrophobicity of this protein. On the other hand, carbonic anhydrase had little effect on ANS fluorescence. Data obtained with the latter two control proteins indicate the sensitivity of ANS fluorescence to exposed hydrophobic surface on proteins, and its suitability for study of lipid-free apoA-I. Since human apoA-I exists predominantly as a monomer at the concentration employed in this experiment (17, 19), the similar level of ANS fluorescence enhancement observed suggests human and chicken apoA-I adopt similar global folds to achieve sequestration of hydrophobic lipid binding regions, most likely through intramolecular helix–helix interactions.

**Effect of Trifluoroethanol on ApoA-I Structure.** Far-UV CD spectra in the absence and presence of the lipid mimetic cosolvent trifluoroethanol (TFE) reveal significant differences in the ratio of ellipticity at 222 and 208 nm (22). In other predominantly  $\alpha$ -helical peptides, a 222 nm/208 nm ellipticity ratio of  $\sim$ 1.0 indicates interhelical contacts, such as those present in coiled-coil or helix bundle structures (44–46). Alternately, values in the range of 0.90 indicate an elongated helix with little or no interhelical contacts (45–47). The ratio of 1.02 observed for lipid-free apoA-I in buffer is consistent with an  $\alpha$ -helix bundle organization while the observed decrease in the ratio of ellipticity at 222 nm/208 nm to 0.90 in the presence of 50% TFE (v/v) suggests

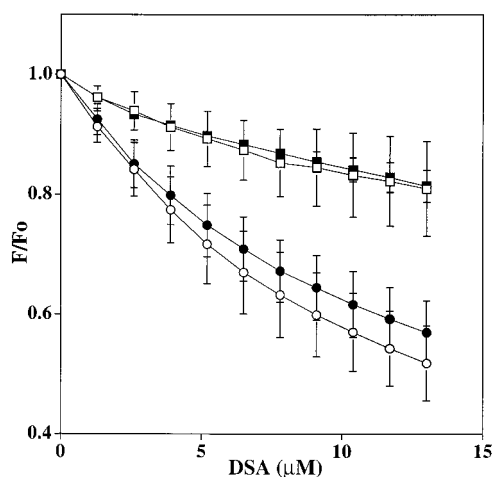


FIGURE 4: Fluorescence quenching of tryptophans by lipid-soluble quenchers. Increasing concentrations of spin-labeled fatty acids: 5-DSA (open circles), 7-DSA (filled circles), 10-DSA (open squares), and 12-DSA (filled squares), were added to 50  $\mu\text{g/mL}$  HDL-bound chicken apoA-I. Fluorescence measurements were conducted at an excitation wavelength of 295 nm (excitation and emission slit widths set at 5 nm), scanning emission from 300 to 450 nm. Relative fluorescence ( $F/F_0$ ) is plotted as a function of quencher concentration.

realignment of apoA-I helices, perhaps by replacement of helix–helix contacts by helix–TFE contacts. In this case, individual helices would no longer be constrained to maintain a bundle configuration. In the present context, we hypothesized that TFE-induced disruption of helix–helix contacts in apoA-I would be reflected in the hydrodynamic properties of the protein. Calculations based on sedimentation velocity experiments reported here reveal a  $s_{20,w}^0$  of 2.31 S and an axial ratio ( $a/b$ ) of 3.8 in buffer, in good agreement with earlier studies (22). In the presence of TFE, the calculated  $s_{20,w}^0$  is 2.22 S and the corresponding axial ratio increased to 4.5, suggesting the protein has adopted a more asymmetric average conformation, which may be caused by partial helix bundle opening due to TFE-induced disruption of hydrophobic helix–helix contacts. This interpretation is consistent with the known effects of TFE on *Manduca sexta* apolipoprotein III tyrosine fluorescence, which are similar to changes which occur upon binding to lipid (48, 49).

**Lipid-Based Quenchers.** Spin-labeled fatty acids were employed as lipid-soluble quenchers to determine the average depth of penetration of W74 and W107 into the surface monolayer of spherical HDL particles. Using a series of DOXYL fatty acids in which the DOXYL moiety is located at different positions along the acyl chain, the depth of binding of apoA-I tryptophan residues was monitored (50). An advantage of the present system is the ability to employ natural chicken HDL directly, since a uniform population of particles containing apoA-I as practically the sole apolipoprotein component can be obtained from chicken plasma. Addition of spin-labeled fatty acids to HDL results in partitioning of the quencher into the surface monolayer of the particle. In each case, increasing the quencher concentration resulted in increased quenching of apoA-I tryptophan fluorescence (Figure 4). Comparing  $K_{\text{app}}$  values, the data show that 5-DSA is the most effective quencher followed by 7-, 10-, and 12-DSA (Table 3). These data are consistent with the hypothesis that HDL-associated apoA-I presents the hydrophobic face of helices containing W74 and W107 to

Table 3: Apparent Stern–Volmer Constants ( $K_{\text{app}}$ ) for Lipid-Soluble Quenchers

quencher	$K_{\text{app}} (\times 10^{-4} \text{ M}^{-1})^{a,b}$
5-DSA	$7.5 \pm 0.9$
7-DSA	$6.0 \pm 0.8$
10-DSA	$2.3 \pm 0.5$
12-DSA	$1.7 \pm 0.1$

<sup>a</sup> Apparent Stern–Volmer quenching constants ( $K_{\text{app}}$ ) for lipid-soluble quenchers of HDL-bound apolipoprotein A-I tryptophan fluorescence were calculated as described under Experimental Procedures. <sup>b</sup> Values reported represent the mean  $\pm$  SD of three independent measurements.

the lipoprotein surface. Furthermore, W74 and W107 do not appear to penetrate deeply into the HDL surface monolayer, a property which may be related to the ability of apoA-I to interact reversibly with lipoprotein surfaces.

## DISCUSSION

A unique feature of amphipathic exchangeable apolipoproteins is an ability to exist stably in lipid-free and lipid-associated states. This property is related to their ability to transfer among lipoprotein particles and, in the case of apoA-I, to serve as progenitor of nascent lipoprotein particle assembly. ApoA-I is particularly interesting in this regard because of the physiological significance of its ability to promote cellular cholesterol efflux as a part of the reverse cholesterol transport pathway (4). At present, however, the molecular basis for the existence of alternate lipid-free and lipid-bound states of apoA-I is not clear. In the present study we have addressed this question through study of apoA-I from chicken plasma. A unique characteristic of this protein is its existence in buffer as a monomer (21, 22) unlike the homologous apoA-I from human plasma (17, 19). The underlying hypothesis of the present study is that lipid-free chicken apoA-I adopts a helix bundle molecular architecture. This hypothesis was evaluated by comparing spectroscopic properties of apoA-I in the absence of lipid as well as in association with phospholipid bilayer disks and spheroidal HDL.

Near-UV CD spectroscopy experiments, which report on the environment of aromatic residues in the protein, revealed dramatic spectral differences between lipid-free and lipid-associated apoA-I. These data can be compared to data reported for human apoA-I (37, 38) and provide evidence for helix repositioning upon interaction with lipid. A difference noted between human and chicken apoA-I in terms of their near-UV CD spectra is that, whereas chicken apoA-I displays a strong negative ellipticity in buffer alone, human apoA-I gives rise to positive ellipticity values between 270 and 288 nm (37). Also, whereas chicken apoA-I ellipticity values decrease dramatically upon lipid interaction, human apoA-I–lipid interaction induced an increase in ellipticity values. Thus, although both proteins display major spectral differences between their respective lipid-free and lipid-bound states, there is no apparent correlation between the changes observed. Support for the conclusion that the changes in both proteins are indicative of a conformational change, however, can be seen from studies of an unrelated  $\alpha$ -helix bundle exchangeable apolipoprotein, *Locusta migratoria* apolipoprotein III, whose X-ray structure has been determined (39). This protein, which possesses two tryptophan residues, also shows a strong negative ellipticity in buffer and a positive ellipticity in lipid.

tophans and lacks both tyrosine and cysteine, displays unusually well-defined near-UV CD spectra (51). Lipid association of this protein, which occurs via conformational opening of the helix bundle (39), gives rise to characteristic changes in near-UV CD spectra, including a complete reversal in the sign of extrema and a 7 nm red shift. When taken together with far-UV CD data indicating chicken apoA-I retains a high content of  $\alpha$ -helix secondary structure in the absence and presence of lipid (Table 1), it is plausible to consider that lipid binding of chicken apoA-I is accompanied by repositioning of  $\alpha$ -helical segments in the protein.

The two tryptophan residues in chicken apoA-I are located in the N-terminal half of the linear protein sequence (positions 74 and 107) and are predicted to reside on the hydrophobic face of distinct amphipathic  $\alpha$ -helices. We have used these intrinsic fluorophores as reporters of local environmental changes which arise from lipid association of the protein. Fluorescence spectra of apoA-I in lipid-free and lipid-bound states were similar, exhibiting a significant blue shift in their corresponding wavelength of maximum emission (excitation 295 nm) compared to free tryptophan. These data indicate that, even in the absence of a lipid surface, W74 and W107 are sequestered from the aqueous environment. Assuming that the blue shift in the lipid-bound states results from interaction of the tryptophan residues with the hydrophobic lipid surface, it is reasonable to conclude that helix-helix interactions in the lipid-free state create a hydrophobic environment in the vicinity of the tryptophan reporter groups.

Tryptophan fluorescence quenching experiments were performed on apoA-I in lipid-free and lipid-bound states. With acrylamide as quencher,  $K_{sv}$  values observed in the different states were comparable, ranging from 1.1 to 1.6  $M^{-1}$  (Table 2). These data indicate that, in the absence of lipid, apoA-I assumes a conformation which shields W74 and W107 from aqueous quenchers to an extent that is similar to lipid-bound apoA-I wherein tryptophan residues are shielded by contact with the lipid milieu.  $Cs^+$  was generally a poor quenching agent, yielding  $K_{sv}$  values of 0.1  $M^{-1}$  in each of the three states. These data indicate that the average accessibility to this positively charged quencher does not change in lipid-free versus lipid-associated apoA-I. In terms of KI quenching of apoA-I tryptophan fluorescence, similar  $K_{sv}$  values were observed for lipid-free and HDL-bound protein. The observed higher  $K_{sv}$  value for DMPC-associated apoA-I provides evidence that the protein adopts a unique conformation in bilayer disk particles versus that in spherical lipoprotein particles.

In other studies, the effects of human apoA-I and chicken apoA-I on ANS fluorescence quantum yield were compared under conditions wherein both proteins are predominantly monomeric in solution. Interestingly, no differences in ANS binding were detected. Stryer (33) showed that ANS binds to hydrophobic regions on proteins, causing a dramatic increase in ANS quantum yield and a significant blue shift in its wavelength of maximum fluorescence intensity. The similar induction of ANS fluorescence observed for human and chicken apoA-I suggests both proteins possess similar amounts of dye-accessible hydrophobic surface. By extension, it is reasonable to consider that human and chicken apoA-I (48% sequence identity) adopt similar global folds

in solution and that structural data obtained on one protein will have implications for the other.

In an effort to examine this aspect in further detail, we conducted studies in the presence of the lipid mimetic cosolvent TFE. TFE has previously been shown to induce additional  $\alpha$ -helix in lipid-free apoA-I, as seen by a significant increase in negative ellipticity, especially at 208 nm (22). Others (44–47) have shown that the ratio of ellipticity at 222 nm to 208 nm can be used to evaluate the existence of interhelical contacts in coiled-coil peptides. Since exchangeable apolipoproteins contain predominantly  $\alpha$ -helical secondary structure, they are suitable candidates for similar analyses. Initially, we compared the ratio of ellipticity at 222 and 208 nm for three monomeric helix bundle exchangeable apolipoproteins whose three-dimensional structures are known [*Locusta migratoria* apoLp-III (39, 51), *Manduca sexta* apoLp-III (40 and unpublished data), and human apoE N-terminal domain (42, 52)]. In these proteins, 208 nm/222 nm ellipticity ratio values approaching 1.0 or above were observed in buffer, in keeping with the fact that they are known to be stabilized by intramolecular helix-helix interactions. In the presence of TFE, these proteins display a decrease in the corresponding ratio, consistent with the concept that TFE effectively disrupts hydrophobic contacts between neighboring amphipathic  $\alpha$ -helices. The observation that chicken apoA-I follows the same pattern provides support for the presence of helix-helix interactions, most likely as an amphipathic  $\alpha$ -helix bundle, in the lipid-free state. To verify that disruption of helix-helix contacts in chicken apoA-I occurs upon introduction of TFE, sedimentation velocity experiments were performed. Calculations based on these data revealed an increase in protein axial ratio ( $a/b$ ) from 3.8 to 4.5 in the presence of 50% TFE (v/v). The formation of a more asymmetric structure in the presence of TFE is conceivably due to partial opening of the helix bundle structure, as a result of replacement of helix-helix contacts in the bundle by helix-TFE contacts, which are not constrained to retain the bundle conformation.

To address questions related to the interaction of apoA-I with the surface of HDL particles, the effect of different lipid-based quenching agents was evaluated. Spin-labeled DOXYL moieties covalently bound to the 5, 7, 10, or 12 position of stearic acid were employed in studies designed to assess the depth of penetration of apoA-I into the surface of HDL. The data indicated that 5-DSA was the best quencher, suggesting that W74 and W107 reside in close proximity to the surface of the lipoprotein. We concluded from these data that chicken apoA-I has a relatively superficial association with the surface of chicken HDL, in general agreement with the ability of apoA-I to interact reversibly with lipoproteins. A recent study showed that another exchangeable apolipoprotein, *M. sexta* apoLp-III, also adopts a superficial location on lipoprotein surfaces (53), although displacement studies show that apoA-I has a higher lipid binding affinity than apoLp-III (54). While it is tempting to speculate that the binding affinity of exchangeable apolipoproteins is not correlated to depth of penetration, it is recognized that the tryptophan reporter groups on apoA-I are localized to specific regions of the protein. It is conceivable that the C-terminus of apoA-I could be responsible for enhanced binding, independent of the N-terminal half which contains the two tryptophan probes (9, 10).



Recently, Borhani et al. (5) reported the crystal structure of human ( $\Delta 1-43$ )apoA-I at 4 Å resolution. The structure revealed a continuously curved, horseshoe-shaped series of 10 amphipathic  $\alpha$ -helices, with 4 truncated apoA-I molecules arranged as pairs of antiparallel dimers. The interaction of molecules A and B to form a stable dimer is due to electrostatic and hydrophobic contacts. The molecular organization of the A/B dimer produces a structure which presents two faces, one predominantly hydrophilic and the other, strongly hydrophobic. Interactions between the hydrophobic surfaces of two dimers stabilize the dimer structure and give rise to the observed tetrameric organization.

On the basis of comparative biophysical studies of full-length apoA-I and ( $\Delta 1-43$ )apoA-I, it has been suggested that the structure reported by Borhani et al. (5) is representative of the conformation of a lipid-bound apoA-I (11). Indeed, it is envisioned that apoA-I dimers, aligned as depicted in the X-ray structure, could form a "belt" around phospholipid bilayer disks or the circumference of spheroidal HDL. It is conceivable that tetramer formation by ( $\Delta 1-43$ )apoA-I in the absence of lipid provides an alternative mechanism to protect the hydrophobic surface of the antiparallel dimers from solvent exposure. By extension, it is plausible that, in the presence of lipid, helix-lipid interactions serve to stabilize the dimer. It is important to recognize that the tetrameric organization observed is not an intermediate state in the lipid binding interactions of apoA-I. Indeed, full-length apoA-I does not adopt a similar lipid-free organization, presumably prevented by virtue of its N-terminal 43 amino acids (11). Whereas the N-terminal deletion induces spontaneous formation of the continuously curved, horseshoe conformation, which is stabilized by intermolecular contacts, full-length apoA-I is induced to undergo a conformational change only as a result of lipid contact.

The data presented in the present study extend this model by providing evidence that apoA-I can adopt a globular amphipathic  $\alpha$ -helix bundle conformation that is stabilized by intramolecular helix-helix interactions. Furthermore, it is clear that lipid contact induces a significant conformational change wherein the molecule replaces helix-helix interactions for helix-lipid interactions. Previous studies of lipid-free human apoA-I (12, 55-57) are also consistent with a helix bundle organization of apoA-I and the concept that lipid binding triggers formation of an altered conformational state that retains its overall  $\alpha$ -helix content yet presents a significant hydrophobic surface to the lipid milieu. Future studies of this intriguing system will be directed toward confirmation that the continuously curved, horseshoe structure reported by Borhani et al. (5) in fact resembles the conformation adopted by full-length apoA-I in the presence of lipid. In addition, further high-resolution structural information is needed to more accurately define the apparent helix bundle organization of apoA-I in the absence of lipid and to distinguish the unique conformations assumed in disk particles and spherical lipoproteins. Success in this endeavor will provide an understanding of the molecular basis for the pivotal role apoA-I plays in the reverse cholesterol transport pathway.

## ACKNOWLEDGMENT

We acknowledge Kim Oikawa for his assistance in CD spectroscopy and fluorescence measurements and Leslie

Hicks for his assistance in sedimentation velocity experiments and preparation of figures. We thank Dr. V. Narayanaswami for her critical reading of the manuscript.

## REFERENCES

1. Brouillette, C. G., and Anantharamaiah, G. M. (1995) *Biochim. Biophys. Acta* 1256, 103-129.
2. Hara, H., and Yokoyama, S. (1991) *J. Biol. Chem.* 266, 3080-3086.
3. Yancey, P. G., Bielicki, J. K., Johnson, W. J., Lund-Katz, S., Palgunachari, M. N., Anantharamaiah, G. M., Segrest, J. P., Phillips, M. C., and Rothblat, G. H. (1995) *Biochemistry* 34, 7955-7961.
4. Fielding, P. E., and Fielding, C. J. (1995) *J. Lipid Res.* 36, 211-228.
5. Borhani, D. W., Rogers, D. P., Engler, J. A., and Brouillette, C. G. (1997) *Proc. Natl. Acad. Sci. U.S.A.* 94, 12291-12296.
6. Gwynne, J., Brewer, H. B., Jr., and Edelhoch, H. (1975) *J. Biol. Chem.* 250, 2269-2274.
7. Rosseneu, M., Van Tornout, P., Lievens, M.-J., Schmitz, G., and Assmann, G. (1982) *Eur. J. Biochem.* 128, 455-460.
8. Holvoet, P., Zhao, Z., Vanloo, B., Vos, R., Deridder, E., Dhoest, A., Taveirne, J., Brouwers, E., Demarsin, E., Engelborghs, Y., Rosseneu, M., Collen, D., and Brasseur, R. (1995) *Biochemistry* 34, 13334-13342.
9. Ji, Y., and Jonas, A. (1995) *J. Biol. Chem.* 270, 11290-11297.
10. Laccotripe, M., Makrides, S. C., Jonas, A., and Zannis, V. I. (1997) *J. Biol. Chem.* 272, 17511-17522.
11. Rogers, D. P., Brouillette, C. G., Engler, J. A., Tendian, S. W., Roberts, L., Mishra, V. K., Anantharamaiah, G. M., Lund-Katz, S., Phillips, M. C., and Ray, M. J. (1997) *Biochemistry* 36, 288-300.
12. Rogers, D. P., Roberts, L. M., Lebowitz, J., Engler, J. A., and Brouillette, C. G. (1998) *Biochemistry* 37, 945-955.
13. Sorci-Thomas, M. G., Curtiss, L., Parks, J. S., Thomas, M. J., and Kearns, M. W. (1997) *J. Biol. Chem.* 272, 7278-7284.
14. Jonas, A., Kezdy, K. E., and Wald, J. H. (1989) *J. Biol. Chem.* 264, 4818-4824.
15. Sparks, D. L., Davidson, W. S., Lund-Katz, S., and Phillips, M. C. (1993) *J. Biol. Chem.* 268, 23250-23257.
16. Dergunov, A. D., Taveirne, J., Vanloo, B., Caster, H., and Rosseneu, M. (1997) *Biochim. Biophys. Acta* 1346, 131-146.
17. Vitello, L. B., and Scanu, A. M. (1976) *J. Biol. Chem.* 251, 1131-1136.
18. Edelstein, C., and Scanu, A. M. (1980) *J. Biol. Chem.* 255, 5747-5754.
19. Formisano, S., Brewer, H. B., Jr., and Osborne, J. C., Jr. (1978) *J. Biol. Chem.* 253, 354-360.
20. Wishart, D. S., Boyko, R. F., Willard, L., Richards, F. M., and Sykes, B. D. (1994) *Comput. Appl. Biosci.* 10, 121-132.
21. Swaney, J. B. (1980) *Biochim. Biophys. Acta* 617, 489-502.
22. Kiss, R. S., Ryan, R. O., Hicks, L. D., Oikawa, K., and Kay, C. M. (1993) *Biochemistry* 32, 7872-7878.
23. Jackson, R. L., Liu, H. U., Chan, L., and Means, A. R. (1976) *Biochim. Biophys. Acta* 420, 342-349.
24. Segrest, J. P., Garber, D. W., Brouillette, C. G., Harvey, S. C., and Anantharamaiah, G. M. (1994) *Adv. Protein Chem.* 45, 303-369.
25. Yokoyama, S., Tajima, S., and Yamamoto, A. (1982) *J. Biochem.* 91, 1267-1272.
26. Jonas, A. (1986) *Methods Enzymol.* 128, 553-582.
27. Greenfield, N. J. (1996) *Anal. Biochem.* 235, 1-10.
28. Homer, R. B., and Alsopp, S. R. (1976) *Biochim. Biophys. Acta* 434, 297-310.
29. Lakowicz, J. R. (1983) in *Principles of Fluorescence Spectroscopy*, pp 44, 257-284, Plenum Press, New York.
30. Lehrer, S. S. (1971) *Biochemistry* 10, 3254-3263.
31. Abrams, F. S., and London, E. (1992) *Biochemistry* 31, 5312-5322.
32. Eftink, M. R., and Ghiron, C. A. (1976) *Biochemistry* 15, 672-680.
33. Stryer, L. (1965) *J. Mol. Biol.* 13, 482-495.

34. Cohn, E. J., and Edsall, J. T. (1943) in *Proteins, Amino Acids and Peptides as Ions and Dipolar Ions*, p 157, Rheinhold, New York.
35. Kuntz, I. D. (1971) *J. Am. Chem. Soc.* 93, 514–516.
36. MacPhee, C. E., Perugini, M. A., Sawyer, W. H., and Howlett, G. J. (1997) *FEBS Lett.* 416, 265–268.
37. Lux, S. E., Hirz, R., Shrager, R. I., and Gotto, A. M. (1972) *J. Biol. Chem.* 247, 2598–2606.
38. Leroy, A., Harms Toohill, K. L., Fruchart, J.-C., and Jonas A. (1993) *J. Biol. Chem.* 268, 4798–4805.
39. Breiter, D. R., Kanost, M. R., Benning, M. M., Wesenberg, G., Law, J. H., Wells, M. A., Rayment, I., and Holden, H. M. (1991) *Biochemistry* 30, 603–608.
40. Wang, J., Gagne, S. M., Sykes, B. D., and Ryan, R. O. (1997) *J. Biol. Chem.* 272, 17912–17920.
41. Wang, J., Narayanaswami, V., Sykes, B. D., and Ryan, R. O. (1998) *Protein Sci.* 7, 336–341.
42. Wilson, C., Wardell, M. R., Weisgraber, K. H., Mahley, R. W., and Agard, D. A. (1991) *Science* 252, 1817–1822.
43. Segrest, J. P., Jones, M. K., De Loof, H., Brouillette, C. G., Venkatachalapathi, Y. V., and Anantharamaiah, G. M. (1992) *J. Lipid Res.* 33, 141–166.
44. Chao, H., Houston, M. E., Jr., Grothe, S., Kay, C. M., O'Connor-McCourt, M., Irvin, R. T., and Hodges, R. S. (1996) *Biochemistry* 35, 12175–12185.
45. Cooper, T. M., and Woody, R. W. (1990) *Biopolymers* 30, 657–676.
46. Lau, S. Y. M., Taneja, A. K., and Hodges, R. S. (1984) *J. Biol. Chem.* 259, 13253–13261.
47. Hodges, R. S., Semchuk, P. D., Taneja, A. K., Kay, C. M., Parker, J. M. R., and Mant, C. T. (1988) *Pept. Res.* 1, 19–30.
48. Narayanaswami, V., Kay, C. M., Oikawa, K., and Ryan, R. O. (1994) *Biochemistry* 33, 13312–13320.
49. Wientzek, M., Kay, C. M., Oikawa, K., and Ryan, R. O. (1994) *J. Biol. Chem.* 269, 4605–4612.
50. Blatt, E., and Sawyer, W. H. (1985) *Biochim. Biophys. Acta* 822, 43–62.
51. Weers, P. M. M., Kay, C. M., Wientzek, M., van der Horst, D. J., and Ryan, R. O. (1994) *Biochemistry* 33, 3617–3624.
52. Fisher, C. A., Wang, J., Francis, G. A., Sykes, B. D., Kay, C. M., and Ryan, R. O. (1997) *Biochem. Cell. Biol.* 75, 45–53.
53. Sahoo, D., Narayanaswami, V., Kay, C. M., and Ryan, R. O. (1998) *J. Biol. Chem.* 273, 1403–1408.
54. Liu, H., Malhotra, V., and Ryan, R. O. (1991) *Biochem. Biophys. Res. Commun.* 179, 734–740.
55. Davidson, W. S., Hazlett, T., Mantulin, W. W., and Jonas, A. (1996) *Proc. Natl. Acad. Sci. U.S.A.* 93, 13605–13610.
56. Nolte, R. T., and Atkinson, D. (1992) *Biophys. J.* 63, 1221–1239.
57. Roberts, L. M., Ray, M. J., Shih, T.-W., Hayden, E., Reader, M. M., and Brouillette, C. G. (1997) *Biochemistry* 36, 7615–7624.

BI982597P